

Study of Polyolefin Gel in Organic Solvents III. Structure and Morphology of Linear Low Density Polyethylene Gel in Organic Solvents[†]

Masaru OKABE, Kazuhiro MITSUI, Fumihiko SASAI,*
and Hideomi MATSUDA*

*Department of Chemical Process Engineering, Faculty of Engineering,
Kanagawa Institute of Technology, 1030, Shimo-ogino, Atsugi,
Kanagawa 243-02, Japan*

** Department of Fine Materials Engineering, Faculty of Textile Science,
Shinshu University, 3-15-1, Tokida, Ueda, Nagano 386, Japan*

(Received October 27, 1988)

ABSTRACT: In order to investigate the structure and morphology of linear low density polyethylene (LLDPE) gel in organic solvents, measurements of gel-melting temperature, melting temperature of crystallites formed in the gel, differential scanning calorimetry, electron microscopy, and shear modulus of the gel have been carried out in a range of concentration from 1 to 20 g/100 cm³. As a result, two kinds of network structures are found to be constructed with increasing concentration of polymer in the gel. That is, one is the network constructed mainly by microcrystallites formed from low molecular weight species with a lot of short chain branches (SCB), whose structure appears in a lower concentration region than *ca.* 4 g/100 cm³; the other is that constructed by crystalline linkages of large crystallites (dendrites) formed from high molecular weight species with a little SCB, which appears in a higher concentration region than 4 g/100 cm³. According to Takahashi's theory derived for gel-melting temperature of crystalline copolymer gel, at least *ca.* 19 ethylene-units participate in the microcrystallite to form a junction point of the network at an early stage of gelation from a solution.

KEY WORDS Sol-Gel Transition / Thermo-Reversible Gel / Polyethylene / Linear Low Density Polyethylene / Morphology / Structure of Gel / Dendrite / Gel-Melting Temperature / Shear Modulus of Gel / Differential Scanning Calorimetry /

It is a well-known phenomenon that some crystalline polymers exhibit thermo-reversible gelation from their dilute or semi-dilute solutions in the vicinity of room temperature. Such gelation is generally recognized to take place as a result of a three-dimensional network formation of flexible polymer chains cross-linked by physical bonds, in which crystallites more or less participate.^{1,2}

Takahashi studied in detail the thermo-

reversible gelation of crystalline polymers from solutions, and proposed the main possibilities of gel-forming agents.^{3,4} That is, a crystalline polymer with copolymeric characters such as chemically different units, stereo-irregularities, geometric isomers, or chain branches is conducive to thermo-reversible gelation from its solution, and junction points of a network of the gel are made up of crystallites. This concept has been widely sup-

[†] Presented in part at the 37th Annual Meeting of the Society of Polymer Science, Japan, May 1988 [*Polym. Prepr. Jpn.*, **37**, No. 4, 844 (1988)] and the 19th Annual Meeting of Union of Chemistry—Related Societies in Chubu Area, Japan, October 1988 [*Prepr.*, **19**, 246 (1988)].

ported by X-ray diffraction and the kinetics as well as thermodynamics of gel-melting behavior of crystallites.

On the other hand, Tan and co-workers⁵ reported that an amorphous polymer, atactic polystyrene (at-Pst), formed a thermo-reversible gel only in certain solvents such as carbon disulfide, *n*-amyl acetate, toluene, or tetrahydrofuran when a solution was cooled from *ca.* -70°C to -150°C , but no gel was formed in cyclohexane, benzene, or decalin. Then, they suggested that the gel formation of at-Pst might involve both chain overlap and network stabilization by chain stiffening or attractive associations of chain segments. In fact, Miyasaka and co-workers⁶ recently reported that an anisotropic structure with sheaf-like shape such as spherulite of crystalline polymers was formed in an at-Pst/CS₂ gel prepared by cooling the solution at -20°C for 48 h. They proposed that a tacticity distribution might exist along each chain, and some segments, where iso or syndio population is rich, gathered together to make small crystalline fragments. However, there still remain unsolved problems in the mechanism of gelation and detailed structures of amorphous and crystalline polymer gels, and at present, such problems are the subject of discussion.

In our previous study,⁷ solutions of linear low density polyethylene (LLDPE), which is a copolymer of ethylene and alkene (α -olefin) such as 1-butene, 4-methyl-1-pentene, or 1-octene, showed thermo-reversible gelation. It

was also found that a large number of crystallites was formed in the gel, and gel-melting temperature depended on solution concentration, molecular weight of the polymer, and the kind of comonomer.

More detailed characterization of LLDPE gel is carried out from viewpoints of thermal properties, morphology, and elastic property in this study.

EXPERIMENTAL

Materials

Four samples of unfractionated LLDPE were used, which were supplied and characterized by Motegi of the Ohita Laboratory, Showa Denko Co. The physical properties of the samples are summarized in Table I. Weight-average molecular weight \bar{M}_w and the number of short chain branches per 1000-methylene groups SCB/1000CH₂ were determined by GPC and ¹³C NMR measurements, respectively. Each sample has the same kind of short chain branching (SCB) derived from a comonomer unit, 1-butene, but each value of \bar{M}_w is different from the others.

Purification of the sample was carried out as follows: Pellets of the sample were dissolved completely in xylene (*ca.* 2 (w/v) %) at its boiling point under a reflux condenser, and then precipitated into an excess of cooled methanol with stirring. After washing with methanol, the sample was sufficiently dried under reduced pressure at 70°C for at least

Table I. Physical properties of linear low density polyethylenes^a

Sample	Density g cm ⁻³	$\bar{M}_w \times 10^{-4}$ (GPC)	Comonomer	SCB/1000CH ₂ (NMR)	T_m^0 °C
LLDPE-1	0.915	11.3	1-Butene	25.3	119.4
LLDPE-2	0.920	10.4	1-Butene	24.3	122.7
LLDPE-3	0.930	7.1	1-Butene	21.0	118.9
LLDPE-4	0.918	5.5	1-Butene	22.5	120.6

^a \bar{M}_w , weight-average molecular weight determined by GPC; SCB/1000CH₂, number of short chain branches per 1000-methylene groups determined by ¹³C NMR; T_m^0 , melting temperature determined by DSC.

48 h. Solvents used were tetralin, benzene, *p*-xylene, and toluene, and purified by the usual method prior to use.

Preparation Method of Gel from Solution

A gel was prepared in a sealed glass tube with *ca.* 35 cm length and 1 cm inner diameter by the following procedure: A definite amount of sample was dissolved completely in a solvent (5 cm³) at an elevated temperature. Then, the sample tube was transferred quickly to a thermobath kept at 25°C, and maintained at 18 h to make a gel.

Measurement of Melting Temperature of Crystallites in Gel by Polarizing Optical Microscope

As reported in the previous study,⁷ large numbers of crystallites are formed in a LLDPE gel. In order to determine the melting temperature of crystallites in the gel, a heating stage for the specimen was designed and constructed in our laboratory.

The melting behavior and melting temperature of crystallites in the gel were successively investigated through an optical microscope at a heating rate of *ca.* 6°C h⁻¹, while the melting process of the crystallites was photographed by a polarized light at various temperatures.

Determination of Gel-Melting Temperature by the Falling-Ball Method

The gel-melting temperature T_m^g was measured by the falling-ball (ball-drop) method described previously,⁷ using a small steel ball of *ca.* 2 mg weight with 0.8 mm diameter. The gel prepared in a sealed glass tube was heated in a thermobath from 25°C at a rate of 6°C h⁻¹, while the height of the steel ball placed on the surface of the gel layer was recorded by a cathetometer as a function of temperature. Then, T_m^g was determined following the previous technique.⁷

Differential Scanning Calorimetry (DSC) of Gel

A DSC measurement of the gel was carried out with a Shimadzu heat flux differential scanning calorimeter, Model DSC-50. A definite amount (20 mg) of gel was put into an aluminum pan, which was then sealed tightly. The temperature was raised from 25°C at a rate of 5°C min⁻¹. Then, a melting temperature region of crystallites in the gel and peak temperatures of the DSC curve were determined as functions of polymer concentration in the gel. Moreover, heat of fusion of the gel was determined through calibration with indium ($T_m = 156.6^\circ\text{C}$, $\Delta H_f = 28.45 \text{ J g}^{-1}$).

Measurement of Static Shear Modulus of Gel

The apparatus for measurement of static shear modulus of gel was constructed in our laboratory. Details of the apparatus were reported in our previous paper.⁸ The measurement was carried out at 25°C. A stainless steel rod contacting with the gel was suspended by a torsion wire. When the torsion wire with a torsion constant Φ was twisted with an angle θ_1 , the stainless steel rod rotated slightly with an angle θ_2 ($\theta_1 > \theta_2$), corresponding to the elasticity of the gel. Then, the angle θ_2 was determined by the lamp-and-scale method.⁹ As the gel was a typical viscoelastic body, the displacement of a laser spot from a reference point on the scale was recorded as soon as possible after the torsion wire was twisted in order to avoid the influence of viscous flow on the shear modulus.

The shear modulus G of gel was calculated by the following Hooke's type equation when the shear strain θ was small⁹:

$$S = G \cdot \theta \quad (1)$$

with

$$S = \Phi(\theta_1 - \theta_2)/2\pi hr_1^2 \quad (2)$$

$$\theta = 2r_2^2\theta_2/(r_2^2 - r_1^2) \quad (3)$$

where S is the shear stress, h is the depth of the

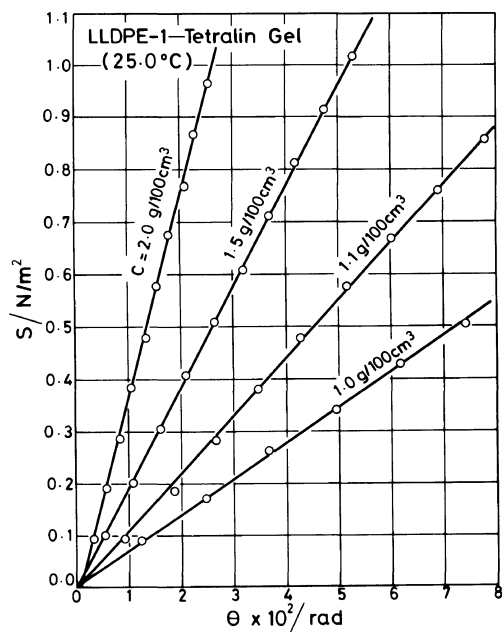


Figure 1. Examples of plots of shear stress S vs. shear strain θ measured at various concentrations C of LLDPE-1-tetralin gels at 25°C, which were constructed by eq 1. The static shear modulus G at each concentration of the gel was determined from a slope of each straight line.

gel contacting the stainless steel rod, r_1 is the radius of the stainless steel rod, and r_2 is the inner radius of a glass container in which the gel is formed.

Examples of the relation between the shear stress S and shear strain θ by eq 1 are shown in Figure 1. An excellent straight line passing through the origin was obtained at each concentration, and thus Hooke's law was applicable to the present crystalline gels. Then, the shear modulus G was determined from the slope of the straight line applying the least-squares method, and the concentration dependence of the shear modulus was investigated.

Observation of Crystallites in Gel by Scanning Electron Microscope (SEM)

The morphology of crystallites in a gel was observed and photographed with an Akashi Model ALPHA-10 scanning electron micro-

scope. The sample preparation for SEM measurements was carried out as follows: After a part of gel was lyophilized, the specimen was coated with a thin layer of gold by the vacuum evaporation technique.

RESULTS AND DISCUSSION

DSC Thermogram of Gel and Melting Temperature of Crystallites in the Gel

Examples of heating DSC curves obtained from LLDPE-3-tetralin gels are shown in Figure 2. The DSC curve of LLDPE-3 (pure sample) had a single endothermic peak at around 119°C, having a broad curve as illustrated with a dashed line. On the other hand, two endothermic peaks lower than 119°C were observed in the case of the gel as seen in the figure. Thus, the melting temperature depression was well recognized. Two endothermic peak temperatures of the gel shifted slightly to higher temperature with increasing concentration of polymer in the gel.

The heat of fusion (enthalpy of fusion) of the gel was determined from the area of the two endothermic curves. These values are summarized in Table II. The data in this table show that the heat of fusion of gel (ΔH_g) increases with increasing polymer concentration C , but *ca.* 163.2 J g⁻¹ (ΔH_s) which is the reduced value to unit gram of LLDPE sample in the gel is obtained without regard to the difference in concentration of polymer. The estimated value of 163.2 J g⁻¹ is closely in accordance with that of 160.2 J g⁻¹ reported by Edwards and Mandelkern¹⁰ from DSC measurement of lamellar crystallites formed in LLDPE (ethylene-butene copolymer) gels in xylene and those formed in dilute solution.

Appearance of such two endothermic peaks is a common property of all gels studied here, suggesting that two kinds of melting processes caused probably by the melting of two kinds of crystalline components exist in the present crystalline gels. On the DSC curves, the gel-melting (sol-gel transition) temperature T_m^g

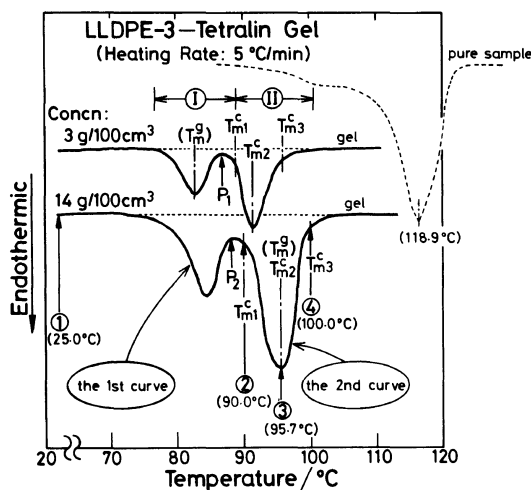


Figure 2. Examples of heating DSC curves obtained from LLDPE-3-tetralin gels with concentrations of 3 and 14 g/100 cm³. Dashed curve is the pure sample. T_m^g shown on the DSC curves is the gel-melting temperature determined by the falling-ball method. $T_{m1}^c - T_{m3}^c$ is the melting temperature region of large crystallites (dendrites) with diameter larger than ca. 5 μ m, whose region was determined by microscopic observation (see Figure 3).

Table II. Values of the heat of fusion of LLDPE-3-tetralin gels^a

C g/100 cm ³	ΔH_g J g ⁻¹	ΔH_s J g ⁻¹
1.1 (C*)	1.84	164.4
3	4.90	163.2
4	6.53	164.8
10	15.19	162.8
14	20.08	159.4
16	23.39	165.3
20	27.78	162.8
Average:		163.2

^a ΔH_g , the heat of fusion per unit gram of gel at each concentration C ; ΔH_s , the heat of fusion per unit gram of LLDPE sample in the gel. C^* shows the minimum solution concentration required for gel formation.

determined by the falling-ball method is marked. An important result is that the T_m^g is nearly in accordance with an endothermic peak temperature of the DSC curve which appeared in

the lower temperature region (the first curve) when the concentration of the gel was less than ca. 4 g/100 cm³. While in the case of gel with higher concentration than 4 g/100 cm³, the T_m^g coincided with that of the second curve as illustrated in the figure. That is, the sol-gel transition took place at the endothermic peak temperature of the first curve when the concentration of the gel was less than 4 g/100 cm³, but took place at that of the second curve if the concentration became higher than 4 g/100 cm³.

When the outside appearance of gel in a glass tube was observed at the temperature of P_1 -point (in the middle of the two endothermic curves) on the DSC curve of 3 g/100 cm³, the gel exhibited turbidity, indicating that crystallites still exist though the sol-gel transition has already occurred at the peak temperature of the first curve. On the other hand, at the P_2 -point on the DSC curve of 14 g/100 cm³, the gel also exhibited considerable turbidity. When the temperature became higher than the P_2 -point, the sol-gel transition took place at the peak temperature of the second curve and the sol became almost transparent near the temperature T_{m3}^c , suggesting that the crystallites have all melted away at T_{m3}^c . It is considered, therefore, that the appearance of two endothermic curves is caused by the melting of two kinds of crystalline components formed in the gel. Moreover, formation of such two crystalline components may be caused by quenching a hot solution of an unfractionated sample having a wide distribution of molecular weight as well as SCB when the gel is prepared. If so, the first curve is concerned with the melting of very small crystallites (microcrystallites) which could not crystallize sufficiently due to molecular species having a lot of SCB. While the second curve is concerned with the melting of crystallites grown somewhat largely.

Recently, Mirabella *et al.*¹¹ and Hosoda¹² studied the structural distribution of LLDPEs, and reported that the DSC curve of a fractionated sample had a single endothermic

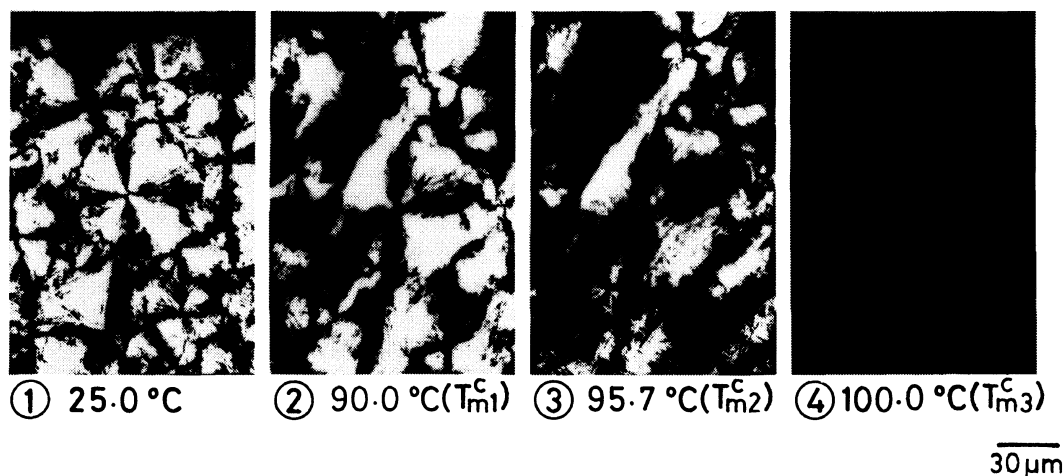


Figure 3. Successive photographs of melting behavior of large crystallites (dendrites) formed in LLDPE-3-tetralin gel at $14 \text{ g}/100 \text{ cm}^3$ under heating of the gel. They were photographed by a polarizing optical microscope with crossed nicols. The number as well as temperature shown below each photograph correspond to those shown on the DSC curve of gel at $14 \text{ g}/100 \text{ cm}^3$ in Figure 2.

peak, while an unfractionated sample had two peaks or a broad one tailing the lower temperature. They suggested that the broad endothermic curve of the sample before fractionation was caused by a broad and multimodal chemical composition distribution of its sample. Moreover, for a series of fractionated LLDPEs, they reported that the number of SCB decreased with increase of molecular weight,^{11,12} and the crystallinity as well as melting temperature of the fractions having comparable molecular weights decreased with increase of SCB.¹² As all present LLDPEs are unfractionated samples, they have a wide distribution of molecular weight ($\bar{M}_w/\bar{M}_n = 2.9\text{--}4.8$) and SCB. Taking the results of Mirabella *et al.* and of Hosoda into consideration, it is plausible that the first endothermic curve of the present gel is caused by melting of small crystallites formed mainly from low molecular weight species having a lot of SCB in the sample. The second curve is caused by melting of large crystallites formed from high molecular weight species having a little SCB.

Determination of Melting Temperature of Crystallites in Gel by Polarizing Optical Microscope

The melting temperature of crystallites in the gel was also determined by another method, *i.e.*, by a polarizing microscope while heating the gel. A heating rate was *ca.* 6°C h^{-1} , which was the same as that of measurement of gel-melting temperature by the falling-ball method. An example of melting behavior of crystallites under heating of LLDPE-3-tetralin gel at $14 \text{ g}/100 \text{ cm}^3$ is shown in Figure 3. They were photographed successively with crossed nicols. The crystallites in the gel do not melt sharply, but gradually as shown in the figure. A melting temperature region of the crystallites thus determined was from T_{m1}^c to T_{m3}^c , whose temperatures are marked on the DSC curves in Figure 2. The T_{m1}^c (see Figure 3(2)) is a starting temperature of the melting of crystallites observable through a polarizing microscope, while the T_{m3}^c is the temperature at which the crystallites have melted away (see Figure 3(4)). T_{m2}^c is the endothermic peak temperature of the second curve. Even at T_{m2}^c ,

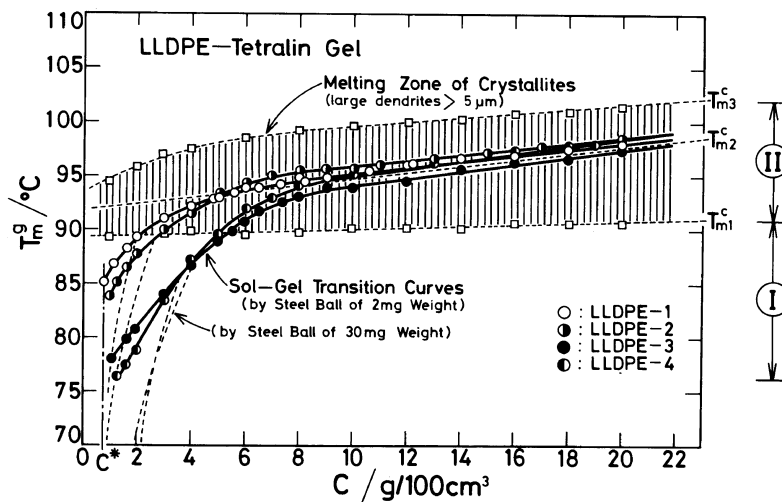


Figure 4. Relation between gel-melting (sol-gel transition) temperature T_m^g and concentration C of LLDPE gels: solid line, the sol-gel transition curve determined by the falling-ball method using a steel ball of 2 mg weight; shaded region ($T_{m1}^c - T_{m3}^c$), the melting temperature region of large crystallites (dendrites) with diameter larger than *ca.* $5 \mu\text{m}$; T_{m2}^c , the endothermic peak temperature of the DSC curve appeared in the region II in Figure 2.

parts of the crystallites still exist as seen in Figure 3(3) though the sol-gel transition has just taken place. In this respect, as referred to by Takahashi,³ the sol-gel transition temperature of a crystalline polymer gel does not coincide with the thermodynamic melting temperature, *i.e.*, the crystal-liquid transition temperature, because the sol still contains crystalline fragments.

The results in Figures 2 and 3 show that a melting temperature region of crystallites ($T_{m1}^c - T_{m3}^c$) determined by the microscopic observation coincides well with the second endothermic curve. Consequently, the second curve is concluded to be caused by the melting of crystallites observable by an optical microscope, *i.e.*, somewhat large crystallites formed probably from high molecular weight species with a little SCB. On the other hand, the first curve of DSC is considered to be caused by the melting of microcrystallites formed from low molecular weight species with a lot of SCB though the melting of microcrystallites could not be observed by the optical microscope. So, in this study, we define a region from T_{m1}^c to

T_{m3}^c as II, while a temperature region lower than T_{m1}^c as I.

Sol-Gel Transition Curve and Dependence of Gel-Melting Temperature on Polymer Concentration and Molecular Weight

The gel-melting temperature T_m^g measured by the falling-ball method and a melting temperature region of crystallites determined by microscopic observation were plotted against polymer concentration. The correlation is shown in Figure 4. In the figure, a shaded region (II) is the melting temperature region of large crystallites which could be observed by a polarizing microscope, while solid lines are the sol-gel transition curves determined by the falling-ball method using a steel ball of *ca.* 2 mg weight.

In our previous studies,^{7,13} a steel ball of *ca.* 30 mg weight was used. However, T_m^g measured by this steel ball lowered abruptly below *ca.* $3 \text{ g}/100 \text{ cm}^3$ as shown in the figure with dashed lines. Thus, the steel ball of 30 mg weight was too heavy to determine precisely the gel-melting temperature below *ca.* $3 \text{ g}/100$

Table III. Values of C^* , T_m^g , and C_0 for linear low density polyethylenes^a

Sample	Tetralin		Benzene		<i>p</i> -Xylene		Toluene		C_0 g/100 cm ³
	C^*	T_m^g	C^*	T_m^g	C^*	T_m^g	C^*	T_m^g	
	g/100 cm ³	°C	g/100 cm ³	°C	g/100 cm ³	°C	g/100 cm ³	°C	
LLDPE-1	0.9	85.2	0.8	78.0	0.9	70.2	0.8	67.5	0.62
LLDPE-2	1.0	84.6	0.8	74.1	1.0	69.6	0.8	67.3	0.65
LLDPE-3	1.1	77.8	1.0	69.5	1.1	67.9	0.9	67.0	0.79
LLDPE-4	1.2	76.5	1.1	68.5	1.2	67.8	1.0	66.8	0.90

^a C^* , the minimum solution concentration required for gel formation; T_m^g , gel-melting temperature at the C^* ; C_0 , the concentration at which quasi-ideal polymer chains begin to overlap with each other in a solution.

cm³. This is the reason why we selected a steel ball of 2 mg weight for measurement of gel-melting temperature in this study.

A melting temperature region from T_{m1}^c to T_{m3}^c of large crystallites is almost the same at each concentration without regard to the difference in samples, but T_{m1}^c and T_{m3}^c increase slightly to higher temperature with increasing concentration of polymer in the gel as shown in Figure 4. The T_m^g of each gel rises successively with increasing polymer concentration, crossing from the region I to II.

In the region I (below *ca.* 4 g/100 cm³) where the sol-gel transition takes place without melting of observable (large) crystallites, it is very characteristic that the T_m^g increases very steeply with increasing polymer concentration. Moreover, the molecular weight dependence of T_m^g appears clearly. That is, the T_m^g increases with increasing molecular weight. However, in the region II (above *ca.* 4 g/100 cm³) where the sol-gel transition takes place accompanying the melting of large crystallites, such molecular weight dependence is not recognized. T_m^g increases very slowly with increasing concentration as well as melting temperature T_m^0 of a pure sample (see Table I) though the difference in T_m^g among the samples is little.

Taking these results into consideration, it is predicted that two kinds of gel states or three-dimensional network structures are constructed in the LLDPE gel below and above the

concentration of *ca.* 4 g/100 cm³.

Critical Gelation Concentration C^ of Gel and Morphology at the C^**

In order to elucidate the mechanism of gelation from a solution, the minimum solution concentration required for gel formation, *i.e.*, the critical gelation concentration C^* , was determined experimentally. Then, C^* was compared with the concentration C_0 at which polymer chains began to overlap with each other in a solution.

The values of C^* , determined by using a steel ball of *ca.* 2 mg weight, are summarized in Table III. The criterion of C^* was taken as the concentration at which the steel ball placed on the surface of gel layer would no longer move downwards. The concentrations C_0 are also listed in Table III. They were estimated approximately by the equation¹⁴⁻¹⁷ $C_0 = kM^{-1/2}$, using the constant $k = 2.1$ given by Takahashi¹⁶ and weight-average molecular weight \bar{M}_w for M . As seen in the table, C^* ranges from 0.8 to 1.2 g/100 cm³, depending slightly on the molecular weight. That is, C^* decreases with increasing molecular weight. Moreover, C^* of each gel is somewhat higher than C_0 , indicating that gelation never takes place merely by the overlap or entanglement of polymer chains.

At the concentration of C^* , many sheaf-like crystallites isolated from one another can be observed as shown in Figure 5(A), which were

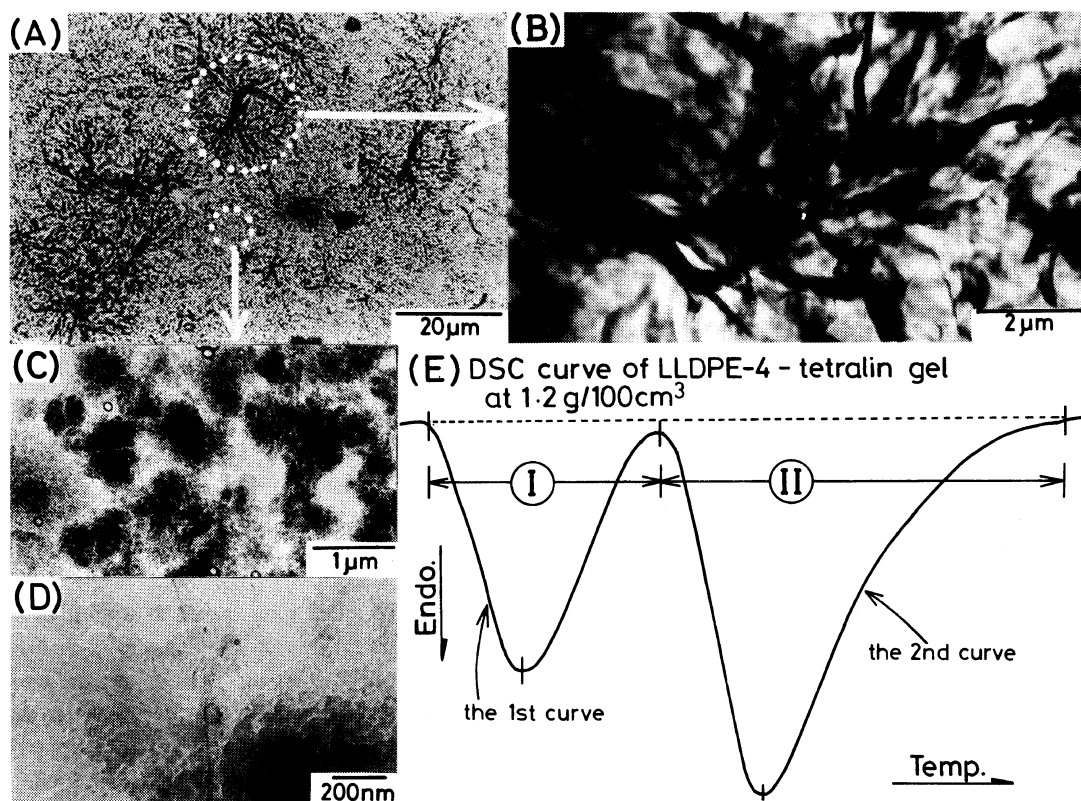


Figure 5. Two kinds of crystalline components ((B) and (C)) formed in LLDPE-4-tetralin gel at the C^* ($1.2 \text{ g}/100 \text{ cm}^3$) and a heating DSC curve of its system (E): (A), sheaf-like (dendritic) crystallites observed by an optical microscope; (B), enlarged morphology of (A) by TEM; (C) and (D), microcrystallites (lamellae) observed by TEM, which are present among the sheaf-like crystallites shown in (A). (D) is the enlarged morphology of (C). These photographs were all obtained from the same specimen placed on a metal grid coated with a thin layer of carbon.

photographed through an optical microscope after the gel was lyophilized. There is a wide distribution of crystallite size ranging from *ca.* 5 to 10 μm . Figure 5(B) is a close-up of the tip of a crystallite seen in Figure 5(A), which was observed by a transmission electron microscope (TEM). It is found from Figure 5(B) that the sheaf-like crystallite is composed of many lamellar crystallites developed like a ribbon, which are twisted.

From measurement of melting temperature of crystallites under heating of gel using a polarizing microscope, the second curve of the DSC shown in Figure 5(E) was concluded to be caused by the melting of sheaf-like crys-

tallites in Figure 5(A). However, the sol-gel transition did not take place at the second curve, but did so near the peak temperature of the first curve. It is expected, therefore, that microcrystallites which cause the first curve accompanying the sol-gel transition coexist with the sheaf-like crystallites. The presence and morphology of microcrystallites were investigated by TEM, and very small lamellar crystallites smaller than 1 μm (see Figure 5(C) and 5(D)) were observed among the sheaf-like crystallites. The morphology of crystallite in Figure 5(C) is considerably different from that in Figure 5(B), *i.e.*, the former is spherulitic, while the latter is dendritic though both of

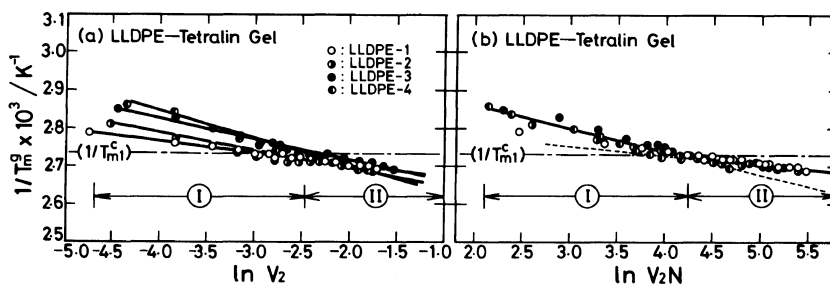


Figure 6. Plots of $1/T_m^g$ vs. $\ln V_2$ (a), and of $1/T_m^g$ vs. $\ln V_2 N$ (b) for LLDPE-tetralin gels, which were constructed using the data shown in Figure 4: (a), by eq 4 (Eldridge-Ferry's plot); (b), by eq 5 (Takahashi-Nakamura-Kagawa's plot). The ordinate ($1/T_m^g$) of each graph has the same scale.

them are essentially composed of lamellae.

It is concluded, therefore, that the gel includes two kinds of crystalline components with different morphology. The melting of lamellar microcrystallites is considered to cause the first endothermic curve in Figure 5(E), which accompanies the sol-gel transition. That is, the three-dimensional network of the LLDPE gel in the vicinity of C^* is constructed mainly by such microcrystallites.

Application of Gel-Melting Temperature T_m^g to Empirical Relationship of Eldridge-Ferry and Theoretical Equation of Takahashi, Nakamura, and Kagawa

Eldridge and Ferry¹⁸ derived empirically the following useful relation between absolute gel-melting temperature T_m^g [K] and volume fraction of a polymer V_2 in a gel, assuming that at least two cross-links per polymer chain are required for the formation of a three-dimensional network:

$$\ln V_2 = \text{const.} + \Delta H_m / RT_m^g \quad (4)$$

where ΔH_m is the heat absorbed on formation of one mol of junction points and R is the gas constant.

According to eq 4, a plot of $\ln V_2$ vs. $1/T_m^g$ [K^{-1}] should give a straight line. Examples of this plot are illustrated in Figure 6(a). Good straight lines are obtained for respective gels. It is obvious that in region I, the molecular weight dependence of T_m^g can be well recogniz-

ed. In region II, however, the difference in T_m^g among samples becomes very small and the molecular weight dependence of T_m^g disappears, corresponding just to the results shown in Figure 4. Considering the linear relationship obtained from the plot by eq 4, the present data phenomenologically satisfy well the Eldridge-Ferry's relation. Moreover, the concentration dependence of gel-melting temperature can be represented well by this type of plot. However, as pointed out by Takahashi,³ the thermodynamics as well as kinetics of the sol-gel transition are not taken into consideration for eq 4 from the standpoint of crystallization.

As seen in Figure 4, the gel-melting temperature T_m^g does not coincide with the thermodynamic melting temperature T_{m3}^c , *i.e.*, $T_{m3}^c > T_m^g$, though the T_m^g coincides nearly with an endothermic peak temperature T_{m2}^c . Taking into account this fact, Takahashi and co-workers³ derived the thermodynamic theory for the gel-melting temperature of a crystallite from the melting temperature depression of a copolymer-diluent system as formulated by Flory¹⁹ and Mandelkern,²⁰ assuming the cross-linking junction point of the gel to be a crystallite comprised of ζ units in length and ρ crystalline sequences in cross section. The theory is written as follows:

$$\frac{1}{T_m^g} = \frac{\zeta}{\zeta \Delta h_u + \zeta B' V_A - 2\sigma_{ec}} \times \left(\frac{\Delta h_u}{T_m^0} + \frac{R V_A}{V_1} - R \ln X_A \right) - \frac{R}{\zeta \Delta h_u + \zeta B' V_A - 2\sigma_{ec}} \ln V_2 N \quad (5)$$

where T_m^g [K] is the observed gel-melting temperature, ζ is the number of repeating units (*i.e.*, ethylene-unit length) in a crystallite, Δh_u [J mol⁻¹] is the heat of fusion of an ethylene unit, B' [J cm⁻³] is the cohesive energy density defined by $\chi_1 = B' V_1 / RT$, χ_1 is the thermodynamic (Flory-Huggins) interaction parameter between the polymer and solvent, V_1 and V_A [cm³ mol⁻¹] are the molar volumes of the solvent and crystalline unit, respectively, σ_{ec} [J mol⁻¹] is the end interfacial free energy per crystalline sequence, T_m^0 [K] is the equilibrium melting temperature of a pure polymer, X_A is the mole fraction of crystalline units, V_2 is the volume fraction of the polymer in the gel, and N is the weight-average degree of polymerization.

The Takahashi's theory indicates that plots of $1/T_m^g$ vs. $\ln V_2 N$ yield a straight line irrespective of differences in molecular weights of the samples, if the values of the molecular and thermodynamic parameters involved in eq 5 are the same for respective samples in a solvent. As the present samples all have the same kind of comonomer, it is expected that the plots by eq 5 for respective samples give a common straight line in an identical solvent.

An example of the plot is shown in Figure 6(b). As expected, a common line is obtained without regard to differences in molecular weights of the samples. However, the line bends at a certain temperature in contrast with the results shown in Figure 6(a). The temperature at the bending point was found just to coincide with the temperature T_{m1}^c shown in Figure 4. That is, the line begins to bend at the temperature where large crystallites observable by an optical microscope begin to melt. This

strongly suggests that two kinds of network structures are constructed below and above the temperature T_{m1}^c , *i.e.*, in regions I and II, respectively.

Concentration Dependence of Static Shear Modulus of Gel

Measurement of the elastic property of a gel is one of the useful methods for investigating the structure of a gel, because the elasticity is considered to reflect the network structure of the gel directly. In previous sections, we reported through measurements of gel-melting and crystallite-melting temperatures that two kinds of network structures might be formed in a LLDPE gel with increasing polymer concentration in the gel.

If two such kinds of network structures were surely constructed in the gel, the corresponding behavior should be observed on the elasticity of the gel. Under such an expectation, the concentration dependence of the shear modulus of LLDPE gel is discussed in this section.

It is widely recognized that the shear modulus G of a large number of natural and synthetic polymer gels obeys the following type relation²¹⁻²⁴ as a function of polymer concentration C :

$$G = K \cdot C^n \quad (6)$$

where K and n are constants. So, the present data were applied to eq 6. The concentration dependence of the shear modulus measured at 25°C is shown in Figure 7 as a double logarithmic plot of G and C . Two straight lines with different slopes were obtained for each sample, corresponding to the results shown in Figure 6(b). The concentration at which two lines intersected was determined for each sample, and *ca.* 4 g/100 cm³ was obtained irrespective of the sample.

The shear modulus increases abruptly from *ca.* 4 g/100 cm³. Moreover, the molecular weight dependence is well recognized, *i.e.*, the shear modulus increases with increasing mo-

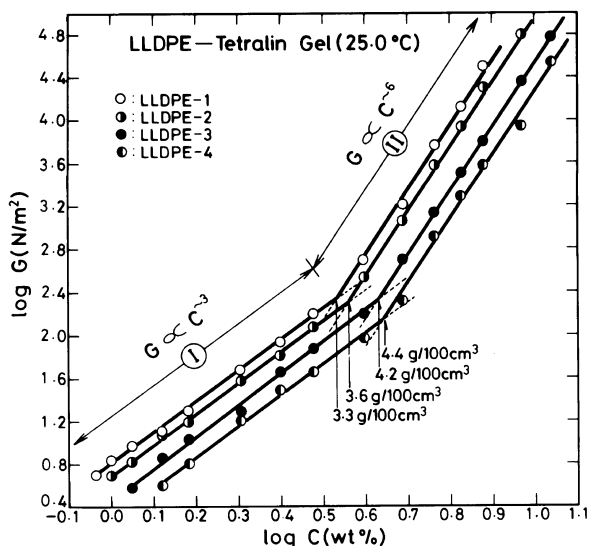


Figure 7. Relation between $\log G$ vs. $\log C$ constructed by eq 6 for LLDPE-tetralin gels at 25°C. An abrupt change of the shear modulus appears from *ca.* 4 g/100 cm³.

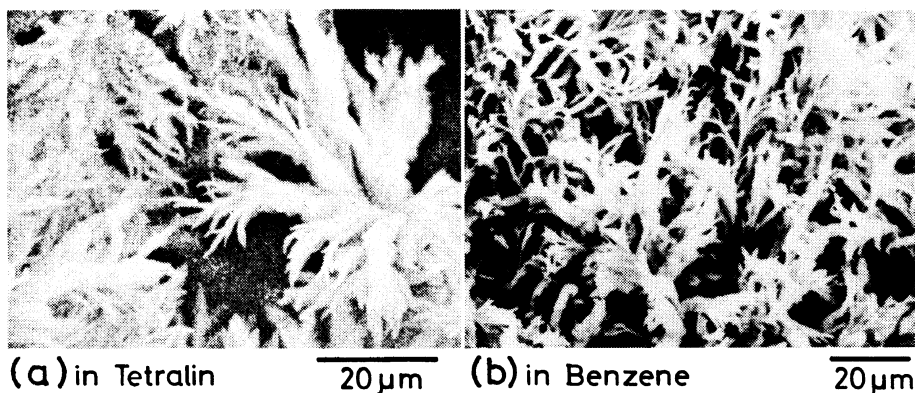


Figure 8. Examples of dendrites observed by SEM: (a), LLDPE-4-tetralin gel at 5 g/100 cm³; (b), LLDPE-4-benzene gel at 5 g/100 cm³.

lecular weight. So, in the figure, we define a concentration region lower than *ca.* 4 g/100 cm³ as I, while a region higher than 4 g/100 cm³ as II. These two regions classified by an abrupt change of the shear modulus are found to be well in accordance with those determined from measurements of DSC, gel-melting temperature, and crystallite-melting temperature as shown in Figure 4. Values of n in eq 6 were determined from slopes of the straight lines,

resulting in *ca.* 3 in the region I and *ca.* 6 in the region II, without regard to differences in molecular weights of the samples.

It was found that the relation of the shear modulus G to the concentration C of the present crystalline gel obeyed a function type of eq 6, but the constant n changed below and above *ca.* 4 g/100 cm³. That is, the structural change of the gel occurred from this concentration. Thus, a three-dimensional network

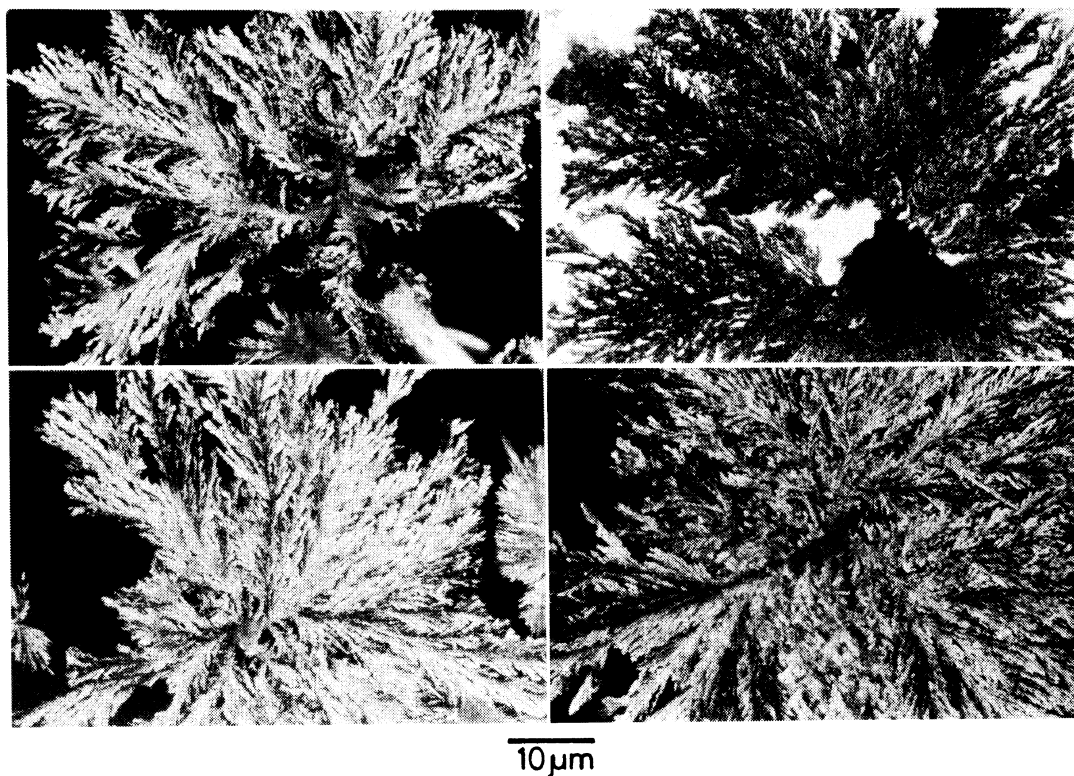


Figure 9. Examples of typical dendrites observed by an optical microscope for LLDPE-4-tetralin gel at $20 \text{ g}/100 \text{ cm}^3$. These dendrites were taken out of the gel by the following technique: A part of the gel was put into an excess of ethanol with stirring. An appropriate amount of water was poured in order to separate the amorphous component from dendrites by differences in densities.

structure of the gel constructed in the region I is concluded to be surely different from that formed in the region II.

Morphology of Crystallites in Gel and Structure of the Gel

The morphology of crystallites formed in a LLDPE gel was observed by SEM. Examples of photographs of the crystallites are shown in Figure 8. They were photographed slightly above the concentration where in Figure 7 two straight lines intersected. The crystallite size (*ca.* $60 \mu\text{m}$) is remarkably larger than that seen in Figure 5, and the development of the crystallite proceeds to a radial direction from its nucleus. Tips of the crystallite grow like a branch of tree, and thus a dendrite is observed.

Moreover, tips of the dendrite link with tips of other dendrites, constructing junction points of a network of the gel. Such large numbers of crystalline linkages among many large dendrites were never observed in the region I where the dendrites were small, and were isolated from one another.

Taking the above results into consideration, the network of the gel in region II is further constructed and strengthened by the participation of stiff linkages among many dendrites grown largely with increasing polymer concentration, in addition to the network made by microcrystallites. The shear modulus of the gel in region II is, therefore, considered to be heightened abruptly as shown in Figure 7, and deviates from a straight line in the region I

with increasing polymer concentration. When the concentration is lower than *ca.* 4 g/100 cm³ (in the region I), the network of the gel is constructed mainly by microcrystallites which are present among sheaf-like crystallites (see Figure 5) or small dendrites isolated from one another. Thus, the sol-gel transition (transition from gel to sol) takes place accompanying the melting of microcrystallites which cause the first endothermic curve, prior to the melting of dendrites which cause the second one.

On the other hand, when the concentration of the gel became higher, some dendrites became an appropriate size so as to contact and link with each other. This may occur at *ca.* 4 g/100 cm³. Then, the network of the gel in the region II is further formed by crystalline linkage of large dendrites, in addition to the microcrystallites. Consequently, in the region II, the sol-gel transition did not take place even after the microcrystallites melted away, but took place accompanying the melting of large dendrites whose melting process could be observed by a polarizing optical microscope (the shaded region in Figure 4).

Detailed Semblance of Dendrite Obtained from Gel with Higher Concentration

From microscopic observation of LLDPE gels with concentrations ranging from C^* to 14 g/100 cm³, many dendrites were found to be formed in the gel, and became larger with increasing polymer concentration. However, the whole shape of the dendrite is not clear. So, more detailed structure of the dendrite was observed.

Examples of photographs of the dendrites formed in LLDPE-4-tetralin gel at 20 g/100 cm³ are shown in Figure 9. They were photographed after washing an amorphous component in the gel away with ethanol. In the figure, a typical dendrite developed just like a branch of tree from the nucleus is observed, and the size is at least larger than *ca.* 90 μm. It is considered to be crystallized from high molecular weight species with a little SCB.

Estimation of Ethylene-Unit Length ζ of Microcrystallite Which Forms Junction Point of Network of Gel by Takahashi's Theory

As seen in Figure 6(b), plots of $1/T_m^g$ vs. $\ln V_2N$ by eq 5 gave a common straight line irrespective of differences in molecular weights of the samples. Consequently, the theory of Takahashi is applicable to the gel-melting temperature of the present LLDPE gel. The ethylene-unit length ζ of a microcrystallite which forms a junction point of network of the gel was estimated for LLDPE-tetralin gels, using the data in the region I in Figure 6(b).

According to eq 5, ζ and σ_{ec} could be estimated from both the intercept and slope of the straight line in region I, if the values of Δh_u , T_m^0 , X_A , and B' were known. The mole fraction of crystalline units X_A was calculated from $X_A = [1 - 0.001(\text{SCB}/1000\text{CH}_2)]$, where SCB/1000CH₂ is the number of short chain branches per 1000-methylene groups (see Table I). The Flory-Huggins interaction parameter χ_1 was determined by the swelling experiment of LLDPE films at 40°C following the method described in the previous study,²⁵ and then the cohesive energy density B' was calculated. The molar volume V_1 of the solvent (tetralin) was calculated from its density. The estimated values were as follows: $X_A = 0.977$, $V_1 = 137.9 \text{ cm}^3 \text{ mol}^{-1}$, $\chi_1 = 0.63$, and $B' = 11.88 \text{ J cm}^{-3}$. The ethylene-unit length ζ in a microcrystallite and the end interfacial free energy per crystalline sequence σ_{ec} were estimated using the values of $\Delta h_u = 8.033 \text{ kJ mol}^{-1}$, $T_m^0 = 418.6 \text{ K}$, and $V_A = 28 \text{ cm}^3 \text{ mol}^{-1}$, which were taken from literature.²⁶

The estimated value of σ_{ec} is 12.64 kJ mol⁻¹. This value is somewhat larger than that of polyethylene single crystal ($\sigma_{ec} = 11.88 \text{ kJ mol}^{-1}$) where chain folding occurs, which was deduced from its dissolution temperature in xylene by Mandelkern.²⁷ The Takahashi's theory indicates that at least *ca.* 19 ethylene-units participate in a microcrystallite to form a junction point of the network of LLDPE-tetralin gels at an early stage of gelation from

a solution, though the multifunctionality ρ of the microcrystallite cannot be estimated from eq 5.

In a preliminary experiment, we examined the gelation ability of random copolymer of ethylene and propylene (EP rubber) in a large number of organic solvents. This sample is widely recognized to show an amorphous property. Needless to say, a homopolymer of ethylene or propylene is a highly crystallizable polymer, and each solution could be easily converted to a thermo-reversible gel at room temperature.^{25,28} However, the amorphous polymer, ethylene-propylene random copolymer, was never converted to a gel at a room temperature. Therefore, the gelation of LLDPE from solution takes place through crystallization of the polymer.

In conclusion, it was found from measurements of thermal and elastic properties of LLDPE gel in organic solvents that two kinds of network structures are constructed in the gel: One is the network formed mainly by microcrystallites existing among small dendrites, whose structure appears below *ca.* 4 g/100 cm³. The other is the network formed by crystalline linkages among dendrites grown largely with increasing concentration, in addition to the network made by the microcrystallites, whose structure appears above *ca.* 4 g/100 cm³.

Judging from the morphology shown in Figure 5(C) or 5(D), the microcrystallite is composed of lamellae. The exact morphology of the microcrystallite in a real gel including a solvent and validity of the estimated size ζ are left for future study.

Acknowledgments. The authors would like to express their sincere appreciation to Professor Dr. Akira Takahashi of the Faculty of Engineering, Mie University, for his useful suggestion and discussion, and to Mr. Yoshihiro Motegi of the Ohita Laboratory, Showa Denko Co., for supplying and characterizing the samples. Thanks are also due to Dr.

Toshio Shigematsu of the Opto-Electronics Laboratory, Nippon Telegraph and Telephone Co. (NTT), for irradiating the polymer films with an electron beam.

REFERENCES

1. P. J. Flory, "Principles of Polymer Chemistry," Cornell University Press, Ithaca, N. Y., 1953, Chapter IX.
2. P. G. de Gennes, "Scaling Concepts in Polymer Physics," Cornell University Press, Ithaca, N. Y., 1979, Part A (Chapter V).
3. A. Takahashi, T. Nakamura, and I. Kagawa, *Polym. J.*, **3**, 207 (1972).
4. A. Takahashi and T. Kato, *Res. Rep. Fac. Eng. Mie Univ.*, **1**, 97 (1976).
5. H.-M. Tan, A. Moet, A. Hiltner, and E. Baer, *Macromolecules*, **16**, 28 (1983).
6. X.-M. Xie, A. Tanioka, and K. Miyasaka, *Polym. J.*, **20**, 93 (1988).
7. M. Okabe, M. Isayama, and H. Matsuda, *Polym. J.*, **17**, 369 (1985).
8. M. Okabe and H. Matsuda, *Rep. Prog. Polym. Phys. Jpn.*, **31**, 49 (1988).
9. For example, T. Nakagawa, *Nippon Kagaku Zasshi*, **72**, 390 (1951).
10. C. O. Edwards and L. Mandelkern, *J. Polym. Sci., Polym. Lett. Ed.*, **20**, 355 (1980).
11. F. M. Mirabella, Jr. and E. A. Ford, *J. Polym. Sci., Part B, Polym. Phys.*, **25**, 777 (1987).
12. S. Hosoda, *Polym. J.*, **20**, 383 (1988).
13. M. Okabe, K. Muto, and H. Matsuda, *Polym. Prepr. Jpn.*, **33**, 936 (1984); M. Okabe, K. Muto, and H. Matsuda, *ibid.*, **34**, 1026 (1985); H. Matsuda, K. Muto, and M. Okabe, *Rep. Prog. Polym. Phys. Jpn.*, **28**, 17 (1985).
14. J. Klein, *Macromolecules*, **11**, 852 (1978).
15. Y. Higo, N. Ueno, and I. Noda, *Polym. J.*, **15**, 367 (1983).
16. M. Kawaguchi, S. Kubota, and A. Takahashi, *Polym. Prepr. Jpn.*, **32**, 1659 (1983).
17. R. C. Domszy, R. Alamo, C. O. Edwards, and L. Mandelkern, *Macromolecules*, **19**, 310 (1986).
18. J. E. Eldridge and J. D. Ferry, *J. Phys. Chem.*, **58**, 992 (1954).
19. P. J. Flory, *J. Chem. Phys.*, **17**, 223 (1949).
20. L. Mandelkern, *J. Appl. Phys.*, **26**, 443 (1955).
21. S. E. Sheppard and S. S. Sweet, *J. Am. Chem. Soc.*, **43**, 539 (1921).
22. J. D. Ferry and P. R. Morrison, *J. Am. Chem. Soc.*, **69**, 388 (1947); J. D. Ferry, *ibid.*, **70**, 2244 (1948).
23. N. Hirai, *Nippon Kagaku Zasshi*, **72**, 837 (1951); N. Hirai and S. Senou, *ibid.*, **75**, 683 (1954).
24. A. G. Ward and P. R. Saunders, "The Rheology of

- Gelatin," in "Rheology (Theory and Applications)," Vol. II, F. R. Eirich, Ed., Academic Press, New York, N. Y., 1958, p 313 (Chapter 8).
25. H. Matsuda, M. Imaizumi, H. Fujimatsu, S. Kuroiwa, and M. Okabe, *Polym. J.*, **16**, 151 (1984).
 26. A. Takahashi, M. Sakai, and T. Kato, *Polym. J.*, **12**, 335 (1980).
 27. J. F. Jackson and L. Mandelkern, *Macromolecules*, **1**, 546 (1968).
 28. M. Okabe and H. Matsuda, *Kobunshi Ronbunshu*, **42**, 397 (1985); H. Matsuda, T. Inoue, M. Okabe, and T. Ukaji, *Polym. J.*, **19**, 323 (1987); H. Matsuda, R. Kashiwagi, and M. Okabe, *Polym. J.*, **20**, 189 (1988).